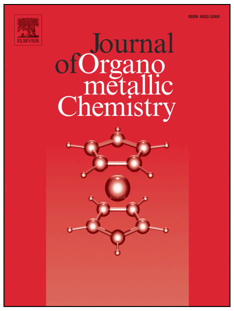

Synthesis and optoelectronic properties of dinuclear cyclometalated platinum (II) complexes containing naphthalene-functionalized carbazole groups in the single-emissive-layer WPLEDs

Zhaoran Hao, Yu Liu, Ying Huang, Fanyuan Meng, Yafei Wang, Hua tan, Shijian Su, Weiguo Zhu

PII: S0022-328X(17)30089-X

DOI: 10.1016/j.jorganchem.2017.02.018

Reference: JOM 19807

To appear in: *Journal of Organometallic Chemistry*

Received Date: 15 November 2016

Revised Date: 3 February 2017

Accepted Date: 12 February 2017

Please cite this article as: Z. Hao, Y. Liu, Y. Huang, F. Meng, Y. Wang, H. tan, S. Su, W. Zhu, Synthesis and optoelectronic properties of dinuclear cyclometalated platinum (II) complexes containing naphthalene-functionalized carbazole groups in the single-emissive-layer WPLEDs, *Journal of Organometallic Chemistry* (2017), doi: 10.1016/j.jorganchem.2017.02.018.

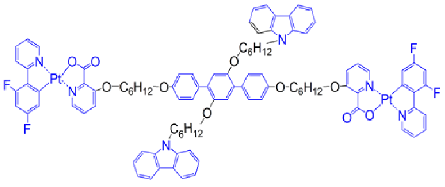

D(FPtpic)C$_6$TPhC$_6$D(dHCz)

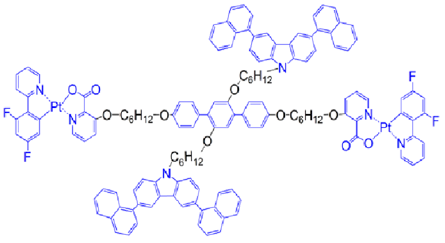

D(FPtpic)C$_6$TPhC$_6$D(dNaCz)

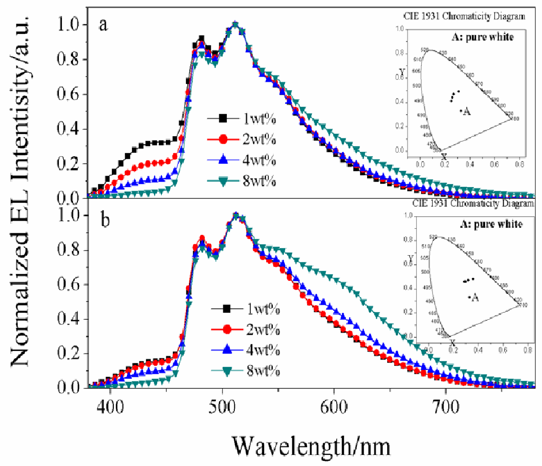

Synthesis and optoelectronic properties of dinuclear cyclometalated platinum (II) complexes containing naphthalene-functionalized carbazole groups in the single-emissive-layer WPLEDs

Zhaoran Hao [a], Yu Liu [a]*, Ying Huang [a], Fanyuan Meng [a,b],
Yafei Wang [a], Hua tan [a], Shijian Su [b]*, Weiguo Zhu [a,c] *

[a] *College of Chemistry, Key Lab of Environment-Friendly Chemistry and Application in Ministry of Education, Xiangtan University, Xiangtan 411105, China*

[b] *State Key Laboratory of Luminescent Materials and Devices, South China University of Technology, Guangzhou 510640, P. R. China*

[c] *School of Materials Science and Engineering, Jiangsu Collaborative Innovation Center of Photovoltaic Science and Engineering, Changzhou University, Changzhou 213164, China*

Email addresses:

(Y. L) liuyu03b@126.com

(S. S) mssjsu@scut.edu.cn

(W. Z) zhuwg18@126.com

ABSTRACT

To tune excimer/aggregation emission and obtain single emissive dopants for white polymer light-emitting diodes (WPLEDs), two novel star-shaped dinuclear cyclometalated platinum (II) complexes, namely DPtF(pic)C_6TPhC_6D(dHCz) and DPtF(pic)C_6TPhC_6D(dNaCz), have been synthesized and characterized, where DPtF(pic) is dinuclear platinum (II) [(4,6-difluorophenyl)-pyridinato-N,$C^{2\prime}$](picolinate) blue-emitting phosphorescent chromophore, D(dHCz) and D(dNaCz) are blue emitting fluorescent chromophores containing carbazole or naphthalene functionalized carbazole group, respectively, TPh is *p*-terphenyl used as central bridging core, finally, each parts of molecular skeleton are wired through nonconjugated hexyloxy ether linkage (C_6). Their thermal, electrochemical and optophysical properties were primarily investigated. The device fabricated with these complexes doped into a host polyvinylcarbazole (PVK) blend with 30 wt % of an electron transport material 1,3-bis-(5-(4-(*tert*-butyl)phenyl)-1,3,4-oxadiazol-2-yl)benzene (OXD-7) showed near-white emission at lower dopant concentration. At 1 wt % dopant concentration, DPtF(pic)C_6TPhC_6D(dHCz) exhibited near-white emission with a luminous efficiency (*LE*) of 1.12 cd/A and a maximum external quantum efficiency (*EQE*) of 0.57% (Commission Internationale de I'Eclairage(CIE) chromaticity coordinates: (0.27, 0.40)) at 2.72 mA/cm^2. At the same dopant concentration, DPtF(pic)-C_6TPhC_6D(dNaCz) showed much tunable near-white emission with a *LE* of 0.99 cd/A and a *EQE* of 0.51% (CIE: 0.30, 0.41) at 0.87 mA/cm^2.

Keywords: Dinuclear cyclomelataed platinum (II) complexes; Blue fluorescent chromophore; Excimer; White organic light-emitting diodes; Synthesis

Introduction

Nowadays, researches on white organic or polymer lighting-emitting diodes (WOLEDs or WPLEDs), pioneered by Kido and his coworkers [1], have drawn particular attention owning to their promising application in flat-panel displays, and solid state lighting sources and back-lighting sources for liquid-crystal displays [2-12]. As a kind of mercury-free illumination light-sources, white OLEDs meet the requirements of the EU WEEE & RoHS directives, besides, from the power consumption point of view, also, WOLEDs/WPLEDs can fully utilize energy converted into light and minimize heat loss [3]. Therefore, much endeavor was made to produce high-efficiency WOLEDs. More encouragingly, the value of efficiency in WOLEDs has broken 90 lm W at 1000 cd/m^2 [7], which surpasses the efficiency of fluorescent bulbs, offering a promising alternative. However, in most studies of WOLEDs, low efficiency and complicated device fabricating remain a tough problem.

Up to now, to obtain efficient WOLEDs/WPLEDs, various strategies have been reported such as doping several fluorescent/phosphorescent emitters into the single-emissive layer (SEL) [13-20], or combining the blue exciplex host and the phosphorescent emitters [21-22], the mutilple-emissive layer (MEL) [23-27], the tandem structures [28-30], the microcavity structures [31-32], and the down-conversion architectures [33], etc. Among these white-emitting devices, the SEL-based WOLEDs/WPLEDs possess a simple process technique and are considered as a class of promising commercial lighting sources. As well known, the white-emitting SEL devices mainly presented two approaches. One is multi-emitters with various emissive colors are used in the same host matrix as the activity layer [34-35], however, this kind of devices always suffer poor color stability as the blue emitter displays a shorter lifetime than the green and red emitters. The other is a single-component emitter with a wide spectral band emission employed in the host matrix as the emitting layer [36-37], obviously, due to simultaneously mixing the intrinsic emission in short-wave region and the aggregate (excimers or electromers) emission in long-wave region, the later SEL devices usually presented white or near-white emission [38-42]. Recently, to further study the formation of the aggregation/excimer and obtain white or near-white emission, there emerging a simple device fabrication process with tunable emission colors through SEL-WOLEDs with single emissive dopant [43-44]. In fact, progress is always coming quickly in making much simpler SEL-WOLEDs with a single emitting component between electrodes have drawn great attention in recent years [45-47]. Furthermore, some SEL-WPLEDs using a series of blue-emitting platinum (II) complexes blended into PVK-PBD host have been reported by our group [48-51], however, their luminous efficiency and brightness, as well as color stability are unsatisfactory.

Inspired by the aforementioned works, to tune excimer emission of platinum (II) complex and get white emission in its doped PLEDs, in this paper, two novel star-shaped dinuclear cyclometalated platinum (II) complexes DPtF(pic)C_6TPhC_6D-(dHCz) and DPtF(pic)C_6TPhC_6D(dNaCz) were synthesized and characterized, in which TPh is *p*-terphenyl used as bridging core, C_6 is a nonconjugated hexyloxy ether linkage, DPtF(pic) is dinuclear platinum (II)

[(4,6-difluorophenyl)-pyridinato-N,$C^{2\prime}$]-(picolinate) blue-emitting phosphorescent chromophore, D(dHCz) and D(dNaCz) are blue emitting fluorescent chromophores containing carbazole or naphthalene functionalized carbazole group, respectively. Both platinum (II) complexes molecular structures are shown in Chart 1 and the synthetic routes of the complexes are shown in Scheme 1. Herein, blue-emitting fluorescent chromophore can enhance blue emission component and carrier-transporting ability of its corresponding platinum (II) complex [50]. Inserting a nonconjugated C_6TPhC_6 group between the fluorescent chromophore and phosphorescent chromophore is expected to efficiently manage intra-molecular energy transfer, and partly to tune the excimer formation as the *p*-terphenyl group C_6TPhC_6 exist a distorted configuration [51]. Moreover, appending naphthalene to the non-planar Cz unit in the platinum (II) complex is expected to not only tune the aggregation emission, but also enhance the blue absorption/emission character of these dinuclear platinum (II) complexes. In fact, the introduction of naphthalene certainly enhanced energy transfer from host to dopant, and more easily to form excimer emission in device. By doping these complexes into a blend of poly(vinylcarbazole) (PVK) and 1,3-bis(5-(4-(*tert*-butyl)phenyl)-1,3,4-oxadiazol-2-yl)benzene (OXD-7) (30 wt %) host matrix in single-dopant SEL PLEDs. As expected, at dopant concentration of 1 wt %, DPtF(pic)C_6TPhC_6D(dHCz)-doped device exhibited near-white emission with luminous efficiency (*LE*) of 1.12 cd/A and a maximum external quantum efficiency (*EQE*) of 0.57% at 2.72 mA/cm^2 and the maximum brightness reached 559 cd/m^2 at 197 mA/cm^2 (CIE : 0.27,0.40). Meantime, at the same dopant concentration,

$DPtF(pic)C_6TPhC_6D(dNaCz)$-doped device showed much tunable near-white emission with a *LE* of 0.99 cd/A and a *EQE* of 0.51% at 0.87 mA/cm^2 and a maximum brightness of 530 cd/m^2 at 234 mA/cm^2 (CIE : 0.30,0.41). In addition, with increasing dopant concentrations from 2 to 8 wt %, the host matrix's emission gradually quenched, and all devices showed pale-green emission with aggregation/excimer and dimer emission character. Therefore, grafting a blue-emitting fluorescent chromophore into a platinum (II) complex with planar structure through a nonconjugated linkage can effectively tune the aggregation/ excimer formation and acquire white emission in SEL-WPLEDs.

Experimental Section

General Measurements

All reactions were performed under purified nitrogen protection and were monitored by thin-layer chromatography (TLC). Flash column chromatography and preparative TLC were carried out using silica gel from Merck (200-300 mesh). All ^{1}H NMR and ^{13}C NMR spectra were acquired at a Bruker Dex-400NMR instrument using $CDCl_3$ as solvent. Mass spectra (MS) were recorded on a Bruker Autoflex TOF/TOF (MALDITOF) instrument using dithranol as a matrix. Elemental analysis was carried out with a Harrios elemental analysis instrument. Thermogravimetric analysis (TGA) was performed under a nitrogen atmosphere at a heating rate of 10 °C/min using a Perkin-Elmer TGA-7 thermal analyzer. UV-vis absorption and fluorescence spectra were recorded with a Shimadzu UV-265 spectrophotometer and a Perkin-Elmer LS-50 luminescence spectrometer, respectively. Cyclic voltammetry was carried out on a CHI660A electrochemical workstation in a conventional three electrode cell using a platinum spar work electrode, a platinum wire counter electrode and KCl saturated Ag/Ag^+ reference electrode, respectively. The CV measurement was performed in a solution of tetrabutylammonium hexafluorophosphate (Bu_4NPF_6) (0.1 M) with a scan rate of 50 mV/s at room temperature (RT) under nitrogen flow protection.

Device Fabrication

EL spectra were recorded with an Insta-Spec IV CCD system (Oriel). Luminance was measured with a Si photodiode and calibrated by a PR-705 spectrascan spectrophotometer (Photo Research). The single-layer PLEDs were fabricated with a structure of ITO/PEDOT (40 nm)/EML (PVK/OXD-7:dopant = 70%/30%:x wt%) (80 nm)/Ba (4 nm)/Al (100 nm), in which indium-tin oxide (ITO) and poly(ethylenedioxythiophene)(PEDOT) are used as the anode and hole-injection layer, as well as lithium fluoride (LiF) and Al are employed as the electron-injection layer and cathode, respectively. The emitting layer consists of the D(FPtpic)-TriPhC6D(dHCz) or D(FPtpic)TriPhC6D(dNaCz) dopant and the PVK/OXD-7 blend host matrix, in which the weight ratio of OXD-7 is 30 %. Doping weight concentrations of platinum (II) complexes vary from 1 wt% to 8 wt%.

*Synthesis of 9-(6-bromohexyl)-3,6-bis(4,4,5,5-tetramethyl-1,3,2-dioxaborolan-2-yl)-9H-carbazole (**4**)*

A mixture of 3,6-dibromo-9-(6-bromohexyl)-9H-carbazole (**3**) (1.00 g, 2.05 mmol), 4,4,5,5-tetramethyl-2-(4,4,5,5-tetramethyl-1,3,2-dioxaborolan-2-yl)-1,3,2-dioxa-borol ane (1.25 g, 4.92 mmol), $PdCl_2(dppf)CH_2Cl_2$ (0.06 g, 0.08 mmol) and potassium acetate (1.6 g, 16.4 mmol) in 30 mL 1,4-dioxane. The mixture was stirred under nitrogen atmosphere at 80°C.for 24 h. After cooled to RT, the mixture was poured into water (100 mL), and then extracted with DCM. The combined Organic layer was dried over anhydrous $MgSO_4$ and filtered. The solvent was removed off by rotary evaporation and the residue was purified by silica gel column chromatography using DCM/EA (20:1; *V/V*) as eluent to obtain a brown solid (0.62 g, 77.3%). ^{1}H NMR (400 MHz,$CDCl_3$, TMS, δ ppm): 8.66 (s, 2H), 7.90 (d, *J* = 8.1 Hz, 2H), 7.38 (d, *J* = 8.2 Hz, 2H), 4.32 (t, *J* = 6.9 Hz, 2H), 3.34 (t, *J* = 6. 7 Hz, 2H), 1.91-1.75 (m, 4H), 1.49-1.43 (m, 4H), 1.38 (m, 12H). MALDI-TOF MS (m/z) for $C_{30}H_{42}B_2BrNO_4$, Calcd: 581.248, Found, 581.122.

*Synthesis of 9-(6-bromohexyl)-3,6-di(naphthalen-1-yl)-9H-carbazole (**5**)*

A mixture of compound **4** (1.00 g, 1.72 mmol), 1-bromonaphthalene (0.86 g, 4.12 mmol), $Pd(PPh_3)_4$ (0.10 g, 0.086 mmol), K_2CO_3 (2 M, 7.0 mL) and THF (20 mL) was refluxed for 24 h under nitrogen atmosphere. After cooled to RT, the mixture was poured into water (100 mL), and then extracted with DCM. The combined Organic layer was dried over anhydrous $MgSO_4$ and filtered. The solvent was removed off by rotary evaporation and the residue was chromatographed on a silica column using PE: DCM = 4: 1 (*V*/*V*) as the eluent to give the compound 5 as a white solid (0.73 g, 73.1%). ^{1}H NMR (400 MHz,$CDCl_3$, TMS, δ ppm): 8.25 (s, 2H), 8.05 (d, *J* = 8.4 Hz, 2H), 7.95 (d, *J* = 8.0 Hz, 2H), 7.97-7.88 (m, 2H), 7.67 (d, *J* = 8.07 Hz, 2H), 7.60-7.57 (m, 6H), 7.52 (t, *J* = 7.3 Hz, 2H), 7.45 (t, *J* = 7.4 Hz, 2H), 4.50 (t, *J* = 7.0 Hz, 2H), 3.46 (t, *J* = 6.6 Hz, 2H), 2.10-2.09 (m, 2H), 1.95-1.92 (m, 2H), 1.63-1.50 (m, 4H). MALDI-TOF MS (m/z) for $C_{38}H_{32}BrN$, Calcd: 581.172, Found, 581.134.

Synthesis of Cz-C$_6$*DBrBC*$_6$*-Cz*

A mixture of compound **1** (1.00 g, 3.03 mmol), 2,5-dibromobenzene-1,4-diol (0.33 g, 1.23 mmol), K_2CO_3 (33%, 3 mL), tetrabutylammonium bromide and toluene (20 mL) was stirred at 90°C for 24 h under nitrogen atmosphere. After cooled to RT, the mixture was poured into water (100 mL), and then extracted with DCM. The combined Organic layer was dried over anhydrous $MgSO_4$ and filtered. The filtrate was evaporated to remove the solvent and the residue was passed through a flash silica gel column using PE:DCM=4:1 (*V*/*V*) as the eluent to give the compound Cz-C$_6$DBrBC$_6$-Cz as a white solid (0.84 g, 89%). ^{1}H NMR (400MHz, $CDCl_3$,TMS), δ (ppm): 8.10 (d, J = 7.7 Hz, 4H), 7.48-7.39 (m, 8H), 7.23 (t, J = 7.2 Hz, 4H), 7.04 (s, 2H), 4.33 (t, J = 6.9 Hz, 4H), 3.90 (t, J = 6.0 Hz, 4H), 1.97-1.88 (m, 4H), 1.81-1.72 (m, 4H), 1.50-1.43 (m, 8H). MALDI-TOF MS (m/z) for $C_{42}H_{42}Br_2N_2O_2$, Calcd: 766.159, Found, 765.986.

Synthesis of Cz-C$_6$*TriBC*$_6$*-Cz*

A mixture of **Cz-C$_6$DBrC$_6$-Cz** (0.50 g, 0.65 mmol), 4-(4,4,5,5-tetramethyl-1,3,2-dioxaborolan-2-yl)phenol (0.35 g, 1.57 mmol), $Pd(PPh_3)_4$ (0.076 g, 0.066 mmol), K_2CO_3 (2 M, 3 mL) and THF (20 mL) was refluxed under stirring for 24 h under nitrogen atmosphere. After cooled to RT, the mixture was poured into water (100 mL), and then extracted with DCM. The combined organic layer was dried over anhydrous $MgSO_4$ and filtered. The filtrate was evaporated to remove the solvent and the residue was passed through a flash silica gel column using PE:EA=3:1 (*V*/*V*) as the eluent to give the compound Cz-C_6TriBC_6-Cz as a white solid (0.20 g, 38.7%). ^{1}H NMR (400MHz, $CDCl_3$,TMS), δ (ppm): 8.10 (d, J = 7.6 Hz, 4H), 7.48-7.36 (m, 12H), 7.23 (t, J = 7.4 Hz, 4H), 6.88 (s, 2H), 6.73 (d, J = 8.2 Hz, 4H), 4.25 (t, J = 7.1 Hz, 4H), 3.85 (t, J = 5.9 Hz, 4H), 1.84-1.81 (m, 4H), 1.63-1.62 (m, 4H), 1.39-1.35 (m, 8H). MALDI-TOF MS (m/z) for $C_{54}H_{52}N_2O_4$, Calcd: 792.393, Found, 792.162.

Synthesis of DNaCz-C_6DBrBC_6-CzDNa

DNaCz-C_6DBrBC_6-CzDNa was synthesized according to the method described in *Synthesis of Cz-C_6DBrBC_6-Cz*. The filtrate was evaporated to remove the solvent and the residue was passed through a flash silica gel column using PE: DCM=3:1 as the eluent to give the compound DNaCz-C_6DBrBC_6-CzDNa as a white solid (0.82 g, 86.3%). ^{1}H NMR (400MHz, $CDCl_3$,TMS), δ (ppm): 8.25 (s, 4H), 8.05 (d, *J* = 8.3 Hz, 4H), 7.94 (d, *J* = 8.0 Hz, 4H), 7.88 (d, *J* = 6.0 Hz, 4H), 7.66 (d, *J* = 7.9 Hz, 4H), 7.60 (s, 4H), 7.58-7.55 (m, 8H), 7.53-7.47 (m, 4H), 7.47-7.41 (m, 4H), 7.11 (s, 2H), 4.49 (t, *J* = 6.9 Hz, 4H), 3.97 (t, *J* = 6.0 Hz, 4H), 2.13-2.02 (m, 4H), 1.89-1.82 (m, 4H), 1.69-1.60 (m, 8H). MALDI-TOF MS (m/z) for $C_{82}H_{66}Br_2N_2O_2$, Calcd: 1270.347, Found, 1270.774.

Synthesis of DNaCz-C_6TriBC_6-CzDNa

DNaCz-C_6TriBC_6-CzDNa was synthesized according to the method described in *Synthesis of Cz-C_6TriBC_6-Cz*. The filtrate was evaporated to remove the solvent and the residue was passed through a flash silica gel column using PE: DCM=1:1 (*V*/*V*) as the eluent to give the compound DNaCz-C_6TriBC_6-CzDNa as a white solid (0.82 g, 86.3%). ^{1}H NMR (400MHz, $CDCl_3$,TMS), δ (ppm): 8.21 (s, 2H), 8.08 (d, J = 8.19 Hz, 4H), 7.95-7.84 (m, 8H), 7.62-7.41 (m, 28H), 6.92 (s, 2H), 6.78 (d, *J* = 7.65 Hz, 4H), 4.39 (t, *J* = 6.9 Hz, 4H), 3.89 (t, *J* = 6.4 Hz, 4H), 1.99-1.92 (m, 4H), 1.74-1.64 (m, 4H), 1.50-1.40 (m, 8H). MALDI-TOF MS (m/z) for $C_{94}H_{76}N_2O_4$, Calcd: 1297.584, Found, 1296.133.

Synthesis of DPtF(pic)C$_6$TPhC6D(dHCz)

A mixture of **Cz-C$_6$TriBC$_6$-Cz** (0.076 g, 0.096 mmol), FPtpicC$_6$Br (**2**) (0.13 g, 0.20 mmol), Cs_2CO_3 (0.62 g, 1.90 mmol), KI and acetone (40 mL) was heated to reflux under stirring for 48 h. After cooled to RT, the mixture was filtered. The collected solid was washed by DCM three times. The combined organic solution was distilled successively under ordinary and reduced pressure. The residue was purified by silica gel column chromatography using DCM:methanol = 50:1 (*V*/*V*) as eluent to give the DPtF(pic)C$_6$TPhC6D(dHCz) as a yellow solid (0.90 g, 46.9%). ^{1}H NMR ($CDCl_3$, 400 MHz, TMS) δ (ppm): 9.19 (d, *J* = 5.6 Hz, 2H), 8.63 (d, *J* = 5.2 Hz, 2H), 8.07 (d, *J* = 7.0 Hz, 4H), 7.99 (d, *J* = 8.0 Hz, 2H), 7.85 (d, *J* = 8.6 Hz, 2H), 7.62 (d, *J* = 8.2 Hz, 2H), 7.50-7.48 (m, 6H), 7.42 (d, *J* = 6.8 Hz, 4H), 7.35 (d, *J* = 7.4 Hz, 4H), 7.17 (t, *J* = 7.4 Hz, 4H), 7.14 (d, *J* = 6.2 Hz, 2H), 6.92-6.88 (m, 8H), 6.63 (t, *J* = 9.5 Hz, 2H), 4.22 (t, *J* = 7.1 Hz, 4H), 4.13 (t, *J* = 6.3 Hz, 4H), 3.92 (t, *J* = 6.7 Hz, 4H), 3.86 (t, *J* = 5.9 Hz, 4H), 1.96-1.84 (m, 4H), 1.84-1.69 (m, 12H), 1.50-1.43 (m, 4H), 1.43-1.38 (m, 12H). ^{13}C NMR (100 MHz, $CDCl_3$, TMS), δ(ppm): 170.03, 163.45, 158.28, 128.14, 150.40, 150.32, 149.99, 149.91, 142.84, 142.35, 141.41, 141.34, 140.44, 140.42, 139.58, 139.56, 130.63, 130.56, 130.30, 130.29, 128.05, 125.62, 125.22, 122.94, 122.85, 122.03, 121.81, 121.67, 121.62, 120.30, 118.75, 116.45, 116.38, 114.10, 108.67, 99.77, 99.54, 99.17, 70.44, 69.50, 67.83, 42.86, 29.32, 29.26, 29.17, 28.80, 26.84, 25.85, 26.71, 25.51. MALDI-TOF MS (m/z) for $C_{100}H_{92}F_4N_6O_{10}Pt_2$, Calcd: 2002.612, Found, 2002.818. Anal. Calcd. for $C_{100}H_{92}F_4Pt_2N_6O_{10}$: C 59.93, H 4.63, N 4.19%. Found: C 59.64, H 4.71, N 4.27%.

Synthesis of DPtF(pic)C_6TPhC6D(dNaCz)

DPtF(pic)C_6TPhC6D(dNaCz) was synthesized according to the method described in *Synthesis of DPtF(pic)C_6TPhC6D(dHCz).* The filtrate was evaporated to remove the solvent and the residue was passed through a flash silica gel column using DCM：THF = 50：1 as the eluent to give the DPtF(pic)C_6TPhC6D(dNaCz) as a yellow solid (0.039 g, 35.5%). ^{1}H NMR ($CDCl_3$, 400 MHz, TMS) δ (ppm): 9.18 (d, *J* = 5.6 Hz, 2H), 8.60 (d, *J* = 5.2 Hz, 2H), 8.21 (s, 4H), 8.01 (d, *J* = 8.1 Hz, 6H), 7.92-7.82 (m, 10H), 7.60 (d, *J* = 8.1 Hz, 4H), 7.52-7.43 (m, 24H), 7.40 (d, *J* = 7.0 Hz, 4H), 7.12 (d, *J* = 6.2 Hz, 2H), 6.93-6.85 (m, 8H), 6.62 (t, *J* = 9.9 Hz, 2H), 4.35 (t, *J* = 6.9 Hz, 4H), 4.04 (t, *J* = 6.3 Hz, 4H), 3.90 (t, *J* = 6.4 Hz, 8H), 1.98-1.92 (m, 4H), 1.88-1.82 (m, 4H), 1.75-1.65 (m, 8H), 1.50-1.42 (m, 16H). ^{13}C NMR (100 MHz, $CDCl_3$, TMS), δ(ppm): 170.08, 163.85, 163.71, 163.46, 163.39, 161.63, 161.49, 161.32, 161.19, 159.05, 158.91, 158.31, 158.07, 150.35, 149.96, 142.90, 142.30, 141.25, 141.04, 140.23, 139.53, 133.97, 132.23, 131.63, 130.77, 130.61,130.31, 128.26, 128.20, 127.98, 127.94, 127.41, 127.20, 126.40, 125.93, 125.69, 125.54, 125.47, 125.05, 122.97, 122.00, 121.86, 121.82, 1212.59, 116.37, 114.67, 114.52, 114.49, 114.11, 108.85, 108.58, 108.40, 108.35, 99.81, 99.54, 99.27, 70.33, 69.49, 67.82, 43.25, 29.72, 29.35, 29.16, 28.90, 26.91, 25.94, 25.72, 25.50. MALDI-TOF MS (m/z) for $C_{140}H_{116}F_4N_6O_{10}Pt_2$, Calcd: 2506.798, Found, 2506.912. Anal. Calcd. for $C_{140}H_{116}F_4Pt_2N_6O_{10}$: C 67.03, H 4.66, N 3.03%. Found: C 67.33, H 4.62, N 3.17%.

Results and Discussion

Synthesis and Characterization

As shown in Scheme 1, intermediates of **1**, **2** and **3** were synthesized according to the published procedures [51-53], respectively. The detailed synthesis and characterization of the other compounds and the platinum (II) complexes are given in the experimental section. Meanwhile, the new compounds in this contribution were fully characterized with ^{1}H NMR, ^{13}C NMR, MALDI-TOF mass spectra and elemental analysis (see Electron Supporting Information, ESI).

Thermal stability

The thermal stability of these platinum (II) complexes were measured by thermal gravimetric analysis (TGA) under a stream of nitrogen atmosphere with a scanning rate of 10 °C/min and their TGA curves are shown in Figure S1 (see supporting information). The decomposition temperature (T_d) correspond to a 5% weight loss value are 240 °C for DPtF(pic)C_6TPhC_6D(dHCz) and 266 °C for DPtF(pic)C_6TPhC_6D(dNaCz), respectively, which indicates that these functionalized platinum (II) complexes present good thermal properties. Particularly, DPtF(pic)C_6TPhC_6D(dNaCz) displays an increasing thermal stability. This is mainly due to the grafting of large conjugated naphthalene unit.

Photophysical properties

The UV-vis absorption spectra of the platinum (II) complexes were measured in dichloromethane (DCM) solution at room temperature (RT) is depicted in Figure 1 and the absorption data are collected in Table 1. The optical properties of intermediate containing the fused aromatic ring and model complex are shown in Figure S2. Compared to the absorption spectra of fluorescent fragments and DPtF(pic) portion, an intense high-energy absorption band at 264 nm and a moderate low-energy absorption band at 300 nm were observed for the spin-allowed $^1\pi$-π^* transitions of the DF and carbazole (Cz) units, respectively. The moderate low-lying absorption bands at 324 nm, 350 nm and 396 nm that probably correspond to the mixture of spin-allowed singlet metal-to-ligand charge transfer (^{1}MLCT), spin-forbidden triplet metal-to-ligand charge transfer (^{3}MLCT) and $^3\pi$-π^* transitions. Compared to DPtF(pic)C_6TPhC_6D(dHCz), DPtF(pic)C_6TPhC_6D-(dNaCz) exhibited an additional wider absorption band at 303 nm, which is attributed to the introduction of the fluorescent chromophores of naphthalene (Na) unit. The enhanced UV absorption is considered to be available to improve the energy-transfer efficiency from the host matrix to the platinum (II) complex in PLEDs [49].

Figure 2 shows the photoluminescent (PL) spectra of the platinum (II) complexes both in DCM solution and neat films at RT, and the corresponding data are summarized in Table 1. In the dilute DCM solution, almost identical PL spectra are observed in both platinum (II) complexes. The typical emission structure peaked at 436 nm and 424 nm are observed for DPtF(pic)C_6TPhC_6D(dHCz) and

$DPtF(pic)C_6TPhC_6D(dNaCz)$, respectively, which are assigned to the electronic transition from $^3MLCT/^3\pi$-π^* to ground state [50]. An efficient energy transfer from fluorescent fragments to DPtF(pic) portion was seen in Figure S2, for the emission spectrum of the former matched well with the absorption range of the later, besides, complexes show separated absorption-emission character, while DPtF(pic) portion seems to have a shortcoming of self-extinction. In their concentration-dependent PL spectra (Figure S3), the above typical emission peaks show gradually bathochromic-shift with increasing concentrations, which can be attributed to different aggregation states under various concentrations [50], and this phenomenon was more obvious in $DPtF(pic)C_6TPhC_6D(dNaCz)$. On the other hand, almost similar PL spectra in their neat films with maximum emission peaks at 445 and 421 nm are observed for $DPtF(pic)C_6TPhC_6D(dHCz)$ and $DPtF(pic)C_6TPhC_6D(dNaCz)$, respectively. Furthermore, a broad long-wave-length emission over 570 nm seems to emanate from excimer of the platinum (II) complexes [57], compared to the $DPtF(pic)C_6TPhC_6D(dHCz)$, $DPtF(pic)C_6TPhC_6D(dNaCz)$ showed much weaker excimer emission. Obviously, introducing naphthyl group into fluorescent chromophores could better tune aggregation emission. This phenomenon implies that introducing an expanded π-conjugation group into plane platinum (II) complexes through a non-conjugated linkage is available to achieve tunable wide-range emission, where exist various emissive characters such as mono-molecular, aggregation/excimer emission.

Electrochemical property

The electrochemical properties of the platinum (II) complexes were investigated by cyclic voltammetry, and the resulting data are listed in Table 1. Only a reversible oxidation potential (E_{ox}) was observed of these platinum (II) complexes, the onset oxidation potentials (E_{ox}) of 1.02 and 1.04 V are observed for DPtF(pic)C_6TPhC_6D(dHCz) and DPtF(pic)C_6TPhC_6D-(dNaCz), respectively. According to the formula of $E_{red} = E_{ox} - E_g$, the reduction potentials (E_{red}) value was estimated by the optical band gaps ($E_{g,film,opt}$) and E_{ox}, where $E_{g,film,opt} = 1240/\lambda_{onset,\ film}$. Therefore, the highest occupied molecular orbit (HOMO) and the lowest unoccupied molecular orbital (LUMO) energy levels (E_{HOMO} and E_{LUMO}) can be calculated using the equation, $E_{HOMO} = -(E_{ox} - 0.10) - 5.1$ eV [54]. The E_{HOMO}/E_{LUMO} values of -5.64/-2.71 eV for DPtF(pic)C_6TPhC_6D(dHCz) and -5.66/-2.73 eV for DPtF(pic)C_6TPhC_6D(dNaCz) are obtained, respectively. Obviously, naphthalene-functionalized carbazole group is responsible for lowering E_{HOMO} and E_{LUMO} values when connected with platinum (II) complex.

Electroluminescent Property

To illustrate electrophosphorescent performance of the platinum (II) complexes, the SEL devices with a configuration of ITO/PEDOT (40 nm)/ platinum (II) complex (x wt%) -PVK/OXD-7 (80 nm)/Ba (4 nm)/Al (100 nm) were fabricated by spin-coating process. Where ITO is used as the anode, poly(ethylendioxythiophene) (PEDOT) is used as the hole-injection layer while Ba/Al is employed as a cathode. The emitting layer consists of the dopant of platinum (II) complexes and host matrix of PVK/OXD-7 blend, where the weight ratio of OXD-7 is 30 % in the blend of

PVK/OXD-7, dopant concentrations of the platinum (II) complexes varied from 1 to 8 wt %, respectively.

The electroluminescent (EL) spectra and their corresponding CIE chromaticity diagrams of the DPtF(pic)C_6TPhC_6D(dHCz)-doped and DPtF(pic)C_6TPhC_6D(dNaCz)-doped devices with different concentration from 1 to 8 wt % at current density of 7.5 mA are presented in Figure 3, and their corresponding CIE data are listed in Table 2. For the sake of convenience, devices based on DPtF(pic)C_6TPhC_6D(dHCz) and DPtF(pic)C_6TPhC_6D(dNaCz) are described as “a” and “b”, respectively. Both complexes exhibit broad emission structures from 350 to 750 nm, where the high-lying emission bands at around 375 ~ 500 nm are mainly attributed to the host emission [55]. Meanwhile, emission bands observed at 480 ~ 510 nm are dominated by a certain degree of aggregation of platinum complexes in the matrix of PVK/OXD-7 blend. The low-lying emission band at around 610 nm is the excimer emission, mostly, excimer formed from the Pt entities in different complexes, as previously reported by our group, intense excimer’s emission can be also observed in complex-doped PLEDs with only one Pt entity [48]. With the increasing of dopant concentrations, the host emission gradually decreased in intensity, while the low-energy aggregation/excimer emission increased, which shows an efficient energy transfer from host to dopant. When the dopant concentration is 8.0 wt%, emission from the PVK-OXD-7 was completely quenched. Interestingly, appending naphthalene unit is propitious to enhance energy transfer from host to dopant, and more easily to form excimer emission in device. Obviously, DPtF(pic)C_6TPhC_6D(dHCz)-doped and

DPtF(pic)C_6TPhC_6D(dNaCz)-doped devices presented near-white emission at 1 wt% doping concentration, respectively. When the dopant concentrations increased from 2 wt% to 8 wt%, the devices preliminary showed pale-green emission.

The typical current density-luminance-voltage (*J-L-V*) characteristics of the platinum (II) complexes-doped SEL PLEDs at dopant concentrations from 1 wt% to 8 wt% are shown in Figure 4, respectively. Meantime, the dependence of *LE-PE-J* curves of the platinum (II) complexes-doped SEL PLEDs are presented in Figure 5, for comparison, the device performances are summarized in Table 2. Turn-on voltage of the devices are observed to increase from 5.8 to 8.0 V for DPtF(pic)C_6TPhC_6D(dHCz), as well as 6.2 to 7.2 V for DPtF(pic)C_6TPhC_6D(dNaCz). This further indicates that the device is mainly operated by the carrier trapping mechanism rather than energy transfer mechanism. Meanwhile, a pale-green emission with a maximum luminance of 649 cd/m^2, a LE of 1.31 cd/A and a power efficiency of 0.59 lm/W was obtained in DPtF(pic)C_6TPhC_6D(dHCz)-doped SEL PLEDs at 2 wt% dopant concentration, Particularly, near-white emissions with a maximum brightness of 559 cd/m^2, a *LE* of 1.12 cd/A and a *PE* of 0.50 lm/W was achieved in the DPtF(pic)C_6TPhC_6D(dHCz)-doped SEL PLEDs at 1 wt % dopant concentration. Meanwhile, at the same dopant concentration, near-white emission was also observed in the DPtF(pic)C_6TPhC_6D(dHCz)-doped same device with a brightness of 530 cd/m^2, a *LE* of 0.99 cd/A and a *PE* of 0.41 lm/W. Furthermore, with increasing dopant concentrations from 2 to 8 wt %, both platinum (II) complexes-doped devices exhibited a decreasing luminance due to their luminescent quenching. For comparison, the device performances are summarized in Table 2 and *EQE-J* characteristics are shown in Figure 6. The maximum *EQE* of 0.66% at a current density of 3.52 mA cm^{-2} is observed in the DPtF(pic)C_6TPhC_6D(dHCz)-doped PLEDs at the dopant concentration of 2 wt %. Also, DPtF(pic)C_6TPhC_6D(dNaCz)-doped PLEDs presented a peak *EQE* of 0.50% at a current density of 0.87 mA cm^{-2} at dopant concentration of 1 wt %. Meanwhile, we note that the *EQE* values also preliminary decreased as the dopant concentrations increased from 2 to 8 wt %. This phenomenon was also observed by our previous work [56], which is related to the concentration quenching. This work implies that incorporating a blue fluorescent chromophore into blue-emitting dinuclear platinum (II) complex through nonconjugated chain bridging is a viable strategy to control aggregation/excimer emissions and obtain white-emitting PLEDs with single dopant.

Conclusions

In summary, we have investigated the photophysical, electrochemical and electroluminescent properties of the two platinum (II) complexes, DPtF(pic)C_6TPhC_6D(dHCz) and DPtF(pic)C_6TPhC_6D(dNaCz), where emission can be tuned by distinct emission together with aggregation/excimer and dimer emission characters. At 1 wt % doping concentration, DPtF(pic)C_6TPhC_6D(dHCz)-doped device exhibited near-white emission with the CIE coordinates of (0.27,0.40) and a *LE* of 1.12 cd/A at 2.72 mA/cm^2. Corresponds to DPtF(pic)C_6TPhC_6D(dNaCz)-doped devices, at the same doping concentration, the PLEDs presented much more near-white emission with the CIE coordinates of (0.31, 0.41) and a *LE* of 0.99 cd/A at 0.87 mA/cm^2. Assuredly, inserting a deep blue fluorescent chromophore with the dual picolinic acid by nonconjugated linkage in a platinum (II) complex could effectively tune the aggregation emission and get white emission in SEL-WPLEDs.

Acknowledgments

This work was supported by the National Natural Science Foundation of China (51273168, 51573154), the Hunan Natural Science Foundation (2015JJ2139), and the key project of Hunan Provincial Education Department (13A102).

Appendix A. Supplementary data

Supplementary data related to this article can be found at xxxxx.

References

1) J. Kido, K. Hongawa, K. Okuyama, K. Nagai, Appl. Phys. Lett. 64 (1994) 815-817.
2) J. J. Kido, M. Kimura, K. Nagai, Science 267 (1995) 1332-1333.
3) H. Sasabe, J. J. Kido, J. Mater. Chem. C. 1 (2013) 1699-1707.
4) K. T. Kamtekar, A. P. Monkman, M. R. Bryce, Adv. Mater. 22 (2010) 572-582.
5) G. M. Farinola, R. Ragni, Chem. Soc. Rev. 40 (2011) 3467-3482.
6) C. Tang, X. D. Liu, F. Liu, X. L. Wang, H. Xu, W. Huang, Macromol. Chem. Phys. 214 (2013) 314-342.
7) S. Reineke, F. Lindner, G. Schwartz, N. Seidler, K. Walzer, B. Lüssem, K. Leo, Nature 459 (2009) 234-238.
8) L. B. Quan, G. D. Yu, W. J. Bin, W. Xi, W. Lei, Z. J. Hua, N. H. Long, P. J. Biao, Acta Phys. Chim. Sin. 31 (2015) 1823-1852.
9) Z. B. Wu, D. G. Ma, Mater. Sci. Eng. R. 107 (2016) 1-42.
10) L. Ying, C. L. Ho, H. B. Wu, Y. Cao, W. Y. Wong, Adv. Mater. 26 (2014) 2459-2473.
11) G. J. Zhou, W. Y. Wong, S. Suo, Journal of Photochemistry and Photobiology C: Photochemistry Reviews. 11 (2010) 133-156.
12) X. L. Yang, G. J. Zhou, W. Y. Wong, J. Mater. Chem. C. 2 (2014) 1760-1778.
13) X. Gong, S. Wang, D. Moses, G. C. Bazan, A. J. Heeger, Adv. Mater. 17 (2005) 2053-2058.

14) W. Y. Hung, L. C. Chi, W. J. Chen, Y. M. Chen, S. H. Chou, K. T. Wong, J. Mater. Chem. 20 (2010) 10113-10119.
15) Y. Yang, T. Peng, K. Ye, Y. Wu, Y. Liu, Y. Wang, Org. Electron. 12 (2011) 29-33.
16) C. J. Zheng, J. Wang, J. Ye, M.F. Lo, X. K. Liu, M. K. Fung, X. H. Zhang, C. S. Lee, Adv. Mater. 25 (2013) 2205-2211.
17) W. Song, I. Lee, J. Y. Lee, Adv. Mater. 27 (2015) 4358-4363.
18) H. B. Wu, G. J. Zhou, J. H. Zou, C. L. Ho, W. Y. Wong, W. Yang, J. B. Peng, Y. Cao, Adv. Mater. 21 (2009) 4181-4184.
19) J. H. Zou, H. Wu, C. S. Lam, C. D. Wang, J. Zhu, C. M. Zhong, S. J. Hu, C. L. Ho, G. J. Zhou, H. b. Wu, W. C. H. Choy, J. B. Peng, Y. Cao, W. Y. Wong, Adv. Mater. 23 (2011) 2976-2980.
20) B. H. Zhang, G. P. Tan, C. S. Lam, B. Yao, C. L. Ho, L. H. Liu, Z. Y. Xie, W. Y. Wong, J. Q. Ding, L. X. Wang, Adv. Mater. 24 (2012) 1873-1877.
21) T. Y. Zhang, B. Chu, W. L. Li, Z. S. Su, Q. M. Peng, B. Zhao, Y. S. Luo, F. M. Jin, X. W. Yan, Y. Gao, H. R. Wu, F. Zhang, D. Fan, J. B. Wang, ACS Appl. Mater. Interfaces. 6 (2014) 11907-11914.
22) T. Y. Zhang, B. Zhao, B. Chu, W. L. Li, Z. S. Su, X. W. Yan, C. Y. Liu, H. R. Wu, Y. Gao, F. M. Jin, F. H. Hou, Sci. Rep. 5 (2015) 10234 1-8.
23) K. S. Yook, S. O. Jeon, J. Y. Lee, K. H. Lee, Y. S. Kwon, S. S. Yoon, J. H. Yoon, Org. Electron. 10 (2009) 1378-1381.
24) Y. Divayana, S. Liu, A. K. K. Kyaw, X. W. Sun, Org. Electron. 12 (2011) 1-7.
25) X. Yang, Y. Zhao, X. Zhang, R. Li, J. Dang, Y. Li, G. Zhou, Z. Wu, D. Ma, W. Y. Wong, X. Zhao, A. Ren, L. Wang, X. Hou, J. Mater. Chem. 22 (2012) 7136-7148.
26) S. Lee, H. Shin, J. J. Kim, Adv. Mater. 26 (2014) 5864-5868.
27) G. P. Tan, S. M. Chen, N. Sun, Y. H. Li, D. Fortin, W. Y. Wong, H. S. Kwok, D. G. Ma, H. B.Wu, L. X. Wang, P. D. Harvey, J. Mater. Chem. C. 1 (2013)

808-821.

28) F. W. Guo, D. G. Ma, Appl. Phys. Lett. 87 (2005) 173510 1-3.
29) H. Kanno, R. J. Holmes, Y. Sun, S. Kenacohen, S.R. Forrest, Adv. Mater. 18 (2006) 339-342.
30) Adams, R. D.; Wong, W. Y. J. Organomet. Chem. 694 (2009) 2712-2716.
31) A. Dodabalapur, L. J. Rothberg, R. H. Jordan, T. M. Miller, R. E. Slusher, J.M. Phillips, J. Appl. Phys. 80 (1996) 6954-6964.
32) H. M. Zhang, H. You, J. W. Shi, W. Wang, S. X. Guo, M. D. Liu, D. G. Ma, Synth. Met. 156 (2006) 954-957.
33) B. C. Krummacher, V. E. Choong, M. K. Mathai, S. A. Choulis, F. So, F. Jermann, T. Fiedler, M. Zachau, Appl. Phys. Lett. 88 (2006) 113506 1-3.
34) H. B. Wu, J. H. Zou, F. Liu, L. Wang, A. Mikhailovsky, G. C. Bazan, W. Yang, Y. Cao, Adv. Mater. 20 (2008) 696-702.
35) S. L. Gong, Y. H. Chen, J. J. Luo, C. L. Yang, C. Zhong, J. G. Qin, D. G. Ma, Adv. Funct. Mater. 2011, 21, 1168-1178.
36) J. Liu, Y. X. Cheng, Z. Y. Xie, Y. H. Geng, L. X. Wang, X. B. Jing, F. S. Wang, Adv. Mater. 2008, 20, 1357-1362.
37) Z. He, W. Y. Wong, X. M. Yu, H. S. Kwok, Z. Y. Lin, Inorg. Chem. 45 (2006) 10922-10937.
38) E. L. Williams, K. Haavisto, J. Li, G. E. Jabbour, Adv. Mater. 19 (2007) 197-202.
39) J. Kalinowski, M. Cocchi, D. Virgili, V. Fattori, J. A. G. Williams, Adv. Mater. 19 (2007) 4000-4005.
40) G. J. Zhou, Q. Wang, C. L. Ho, W. Y. Wong, D. G. Ma, L. X. Wang, Chem. Commun. 24 (2009) 3574-3576.
41) G. J. Zhou, Q. Wang, X. Z. Wang, C. L. Ho, W. Y. Wong, D. G. Ma, L. X. Wang, Z. Y. Lin, J. Mater. Chem. 20 (2010) 7472-7484.

42) G. P. Tan, S. M. Chen, C. H. Siu, A. Langlois, Y. F. Qiu, H. B. Fan, C. L. Ho, P. D. Harvey, Y. H. Lo, L. Liu, W. Y. Wong, J. Mater. Chem. C. 4 (2016) 6016-6026.

43) X. M. Yu, H. S. Kwok, W. Y. Wong, G. J. Zhou, Chem. Mater. 18 (2006) 5097-5103.
44) L. H. Xiong, W. Q. Zhu, N. Wei, J. H. Li, W. B. Sun, X. L. Wu, J. Cao, Z. X. Wang, Org. Electron. 14 (2013) 32-37.
45) J. Luo, X.Z. Li, Q. Hou, J. B. Peng, W. Yang, Y. Cao, Adv. Mater. 19 (2007) 1113-1117.
46) S. Y. Shao, J. Q. Ding, L. X. Wang, X. B. Jing, F. Wang, J. Am. Chem. Soc. 134 (2012) 20290-20293.
47) R. M. Adhikari, L. Duan, L. D. Hou, Y. Qiu, D. C. Neckers, B. K. Shah, Chem. Mater. 21 (2009) 4638-4644.
48) Y. F. Wang, Y. Liu, X. S. Li, H. R. Qi, M. X. Zhu, L. Wang, G. T. Lei, Q. L. Wei, W. G. Zhu, J. B. Peng, Y. Cao, Org. Electron. 11 (2010) 1954-1959.
49) J. Luo, Y. Liu, Q. Chen, D. Y. Shi, Y. Huang, J. T. Yu, Y. F. Wang, Z. Y. Zhang, G. T. Lei, W. G. Zhu, Dalton Trans. 42 (2013) 1231-1237.
50) J. T. Yu, J. Luo, Q. Chen, K. Q. He, F. Y. Meng, X. P. Deng, Y. F. Wang, H. Tan, H. G. Jiang, W. G. Zhu, Tetrahedron 70 (2014) 1246-1251.
51) X. S. Li, Y. Liu, J. Luo, Z. Y. Zhang, D. Y. Shi, Q. Chen, Y. F. Wang, J. He, J. M. Li, G. T. Lei, W. G. Zhu, Dalton Trans. 41 (2012) 2972-2978.
52) H. Xu, Z. F. Xu, Z. Y. Yue, P. F. Yan, B. Wang, L. W. Jia, G. M. Li, W. B. Sun, J. W. Zhang, J. Phys. Chem. C. (112) 2008 15517-15525.
53) W. B. Wu, L. J. Huang, Y. J. Fu, C. Ye, J. G. Qin, Z. Li, Chin. Sci. Bull. 58 (2013) 2753-2761.
54) C. M. Cardona, W. Li, A. E. Kaifer, D. Stockdale, G. C. Bazan, Adv. Mater. 23 (2011) 2367-2371.
55) L. D. Hou, L. Duan, J. Qiao, D. Q. Zhang, L. D. Wang, Y. Cao, Y. Qiu, J. Mater.

Chem. 21 (2011) 5312-5318.

56) Y. Liu, Y. F. Wang, J. He, Q. Q. Mei, K. Chen, J. J. Cui, C. Li, M. X. Zhu, J. B. Peng, W. G. Zhu, Y. Cao, Org. Electron. 13 (2012) 1038-1043.

57) J. Kalinowski, M. Cocchi, L. Murphy, J.A.G. Williams, V. Fattor， Chemical Physics. 2010, 378, 47-57.

Figure and Tables

Chart 1. Molecular structures of platinum (II) complexes.

Scheme 1. Synthetic routes of platinum (II) complexes.

Figure 1. UV-vis absorption spectra of platinum (II) complexes in DCM solution (1.0 $\times 10^{-5}$ M) at RT.

Figure 2. PL spectra of platinum (II) complexes in DCM solution (1.0 $\times 10^{-5}$ M) and neat films at RT.

Figure 3. EL spectra and the CIE coordinates (inset) of platinum (II) complexes-doped PLEDs at dopant concentrations from 1 to 8 wt %, respectively.

Figure 4. The *J-L-V* curves of platinum (II) complexes-doped PLEDs at dopant concentrations from 1 to 8 wt %, respectively.

Figure 5. The *LE-PE-J* curves of platinum (II) complexes-doped PLEDs at dopant concentrations from 1 to 8 wt %, respectively.

Figure 6. The *J-EQE* curves of platinum (II) complexes-doped PLEDs at different concentrations from 1 to 8 wt %, respectively.

Table 1. Photophysical, electrochemical and thermal parameters of platinum (II) complexes.

Table 2. EL parameters of platinum (II) complexes-doped PLEDs.

Chart 1

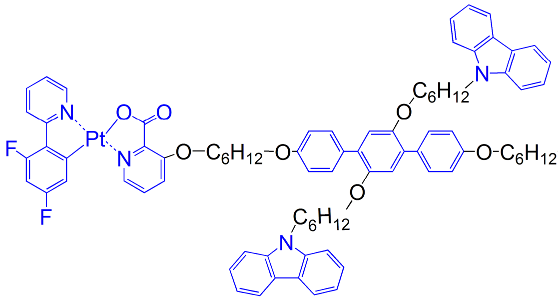

D(FPtpic)C$_6$TPhC$_6$D(dHCz)

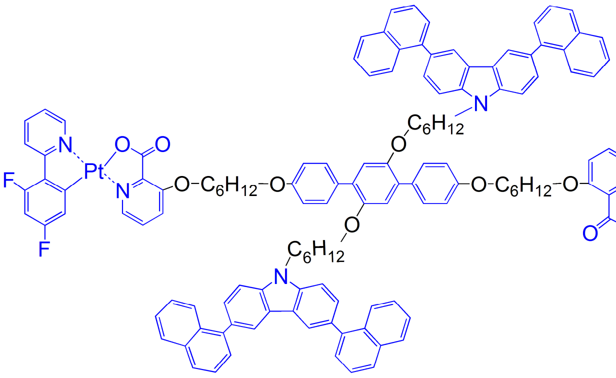

D(FPtpic)C$_6$TPhC$_6$D(dNaCz)

Scheme 1

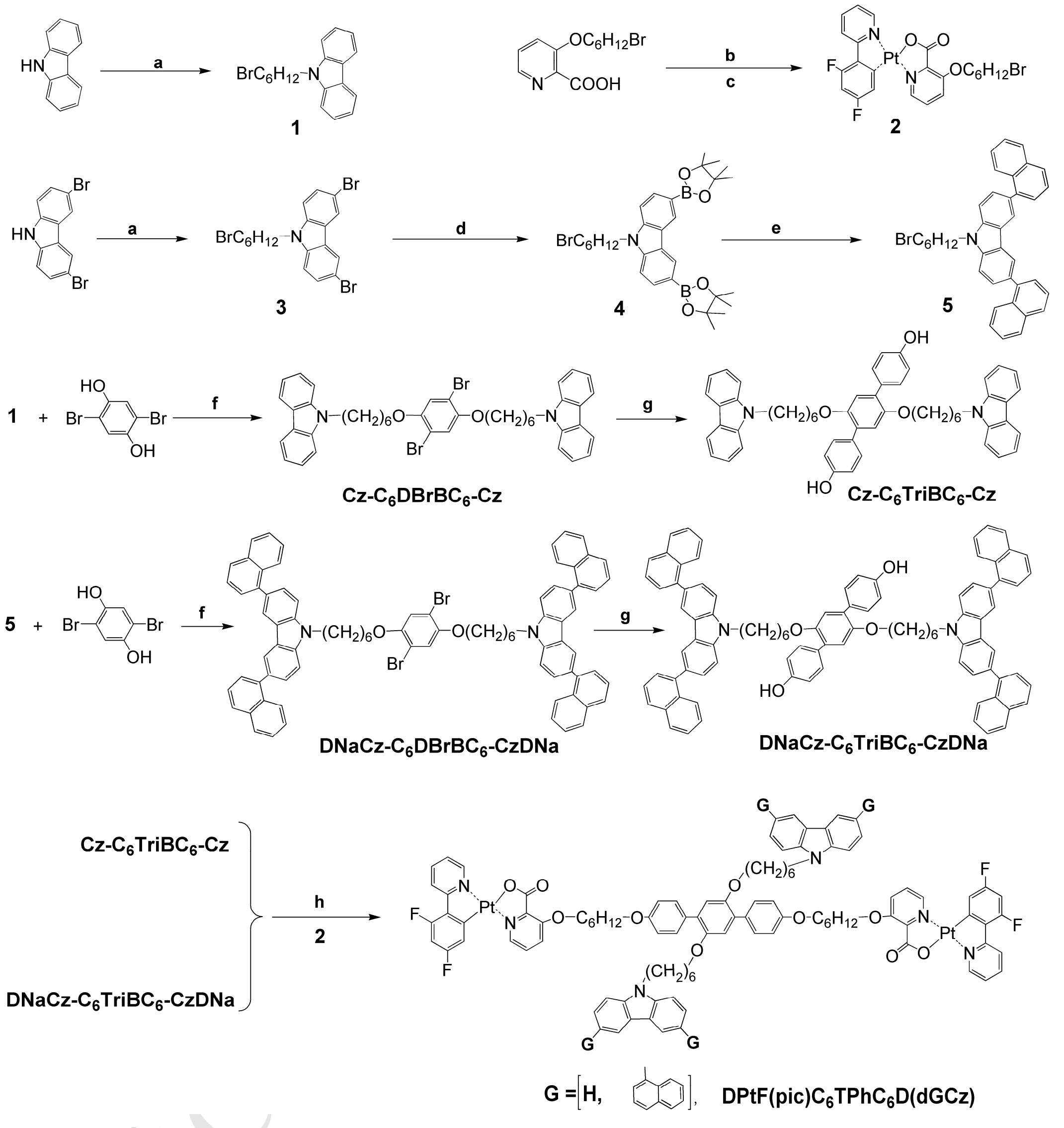

Reaction conditions: (a) K_2CO_3, KI, Acetone, 1,6-dibromohexane; (b) 2-(2,4-difluorophenyl)pyridine, K_2PtCl_4, 2-Ethoxyethanol/Water; (c) Acetylacetone, Na_2CO_3, 2-Ethoxyethanol; (d) $PdCl_2(dppf)CH_2Cl_2$, KOAc, 4,4,5,5-tetramethyl-2-(4,4,5,5-tetramethyl-1,3,2-dioxaborolan-2-yl)-1,3,2-dioxaborolane, 1,4-Dioxane; (e) THF, 1-Bromonaphthalene, $Pd(PPh_3)_4$, K_2CO_3 (2 M); (f) KOH(aq) (35%), Toluene; (g) 4-(4,4,5,5-tetramethyl-1,3,2-dioxaborolan-2-yl)phenol, $Pd(PPh_3)_4$, K_2CO_3 (2M), Toluene; (h) **2**, Cs_2CO_3, KI, Acetone.

Figure 1

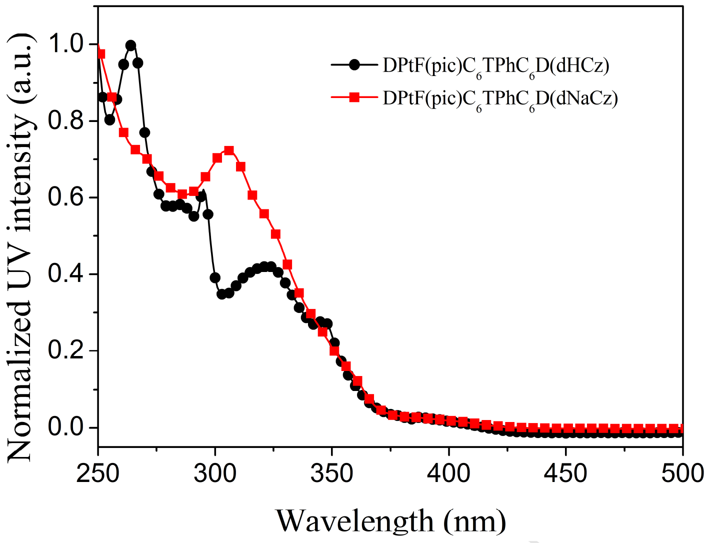

Figure 2

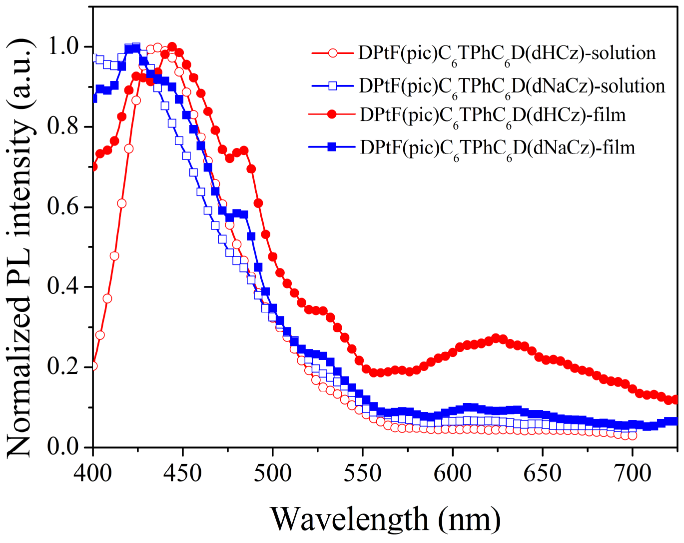

Figure 3

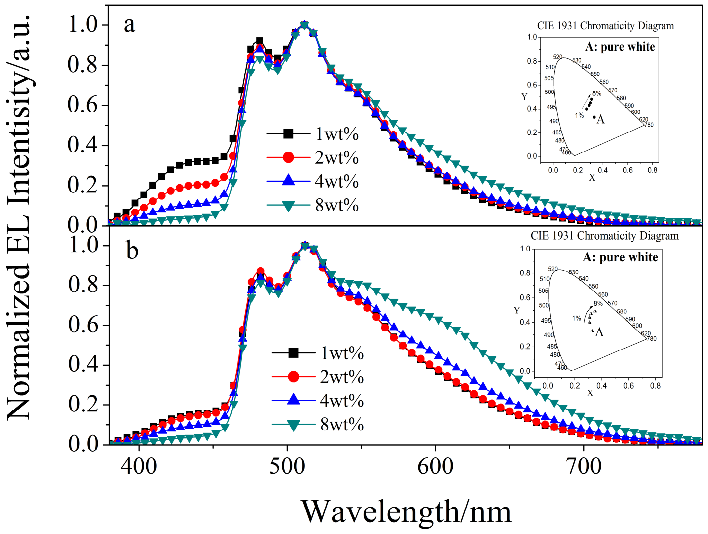

Figure 4

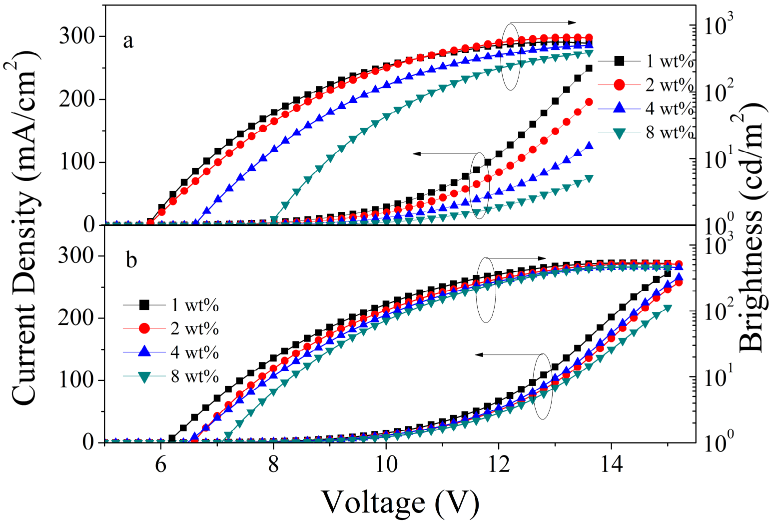

Figure 5

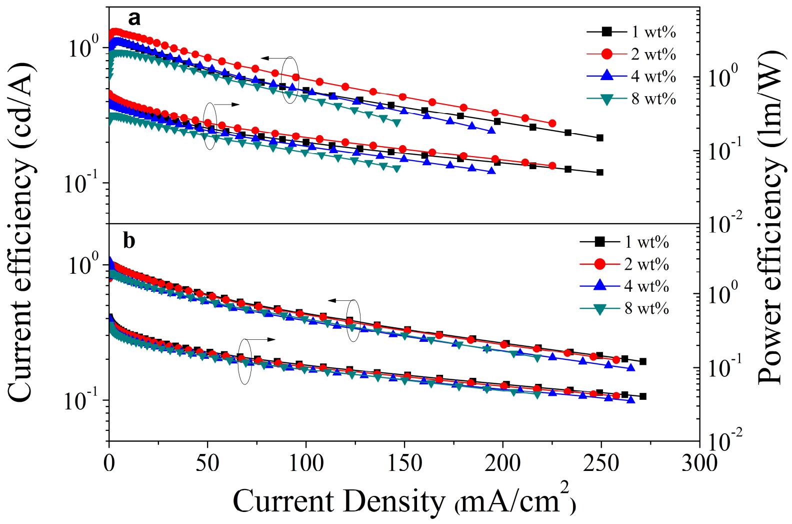

Figure 6

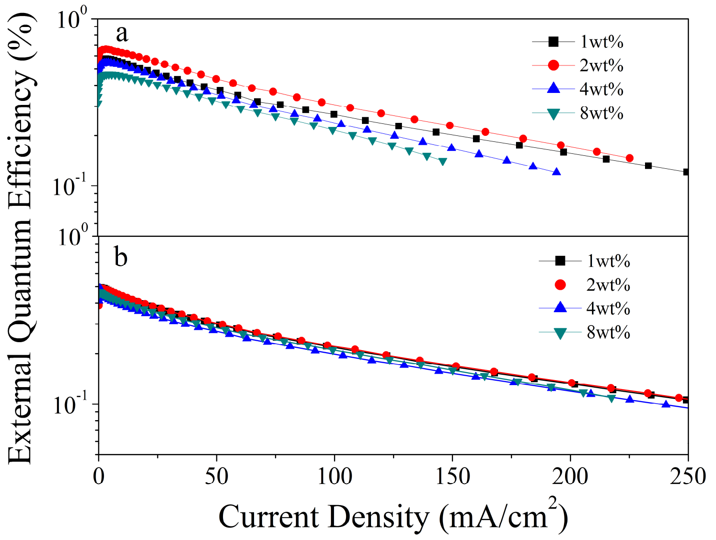

Table 1

Compound [a]	λ_{abs} (nm)	$\lambda_{em}{}^{b}$ (nm)	$\lambda_{em}{}^{c}$ (nm)	E_{ox} (V)	$E_g{}^{d}$ (eV)	E_{HOMO} (eV)	$E_{LUMO}{}^{f}$ (eV)
A	264, 283, 294, 324, 349, 396	436	425, 443, 484, 529, 623	1.02	2.93	-5.64	-2.71
B	267, 303, 323, 395	424	421, 440, 481, 527, 610	1.04	2.93	-5.66	-2.73

[a] A and B instead of DPtF(pic)C_6TPhC_6D(dHCz) and DPtF(pic)C_6TPhC_6D(dNaCz), respectively; [b] Measured in DCM(10^{-5} M) at 298 K; [c] Measured in the neat film at 298 K; [d] Estimated from the onset of low-lying absorption edge; [e] $E_{HOMO} = -(E_{ox} - 0.48) - 5.1$ eV, where 0.48 V is the potential for ferrocene vs. Ag/AgCl and 5.1 eV is the energy level of ferrocene to the vacuum energy level; [f] $E_{LUMO} = E_g + E_{HOMO}$.

Table 2

Dopant (wt%)	[a] V_{on} [nm]	[b] J [mA/cm^2]	Max L [cd/m^2]	[c] J [mA/cm^2]	Max *LE* [cd/A]	Max *PE* [lm/W]	Max *EQE* [%]	*CIE* [*x*, *y*]
A-1	5.8	197	559	2.72	1.12	0.50	0.57	(0.27, 0.40)
A-2	5.8	180	649	2.15	1.31	0.59	0.66	(0.29, 0.43)
A-4	6.6	138	503	3.63	1.09	0.43	0.55	(0.30, 0.45)
A-8	8.0	116	433	4.73	0.92	0.30	0.46	(0.31, 0.48)
B-1	6.2	234	530	0.87	0.99	0.41	0.51	(0.30, 0.41)
B-2	6.6	217	517	1.36	0.99	0.41	0.50	(0.31, 0.43)
B-3	6.6	225	462	0.52	1.05	0.45	0.49	(0.32, 0.46)
B-4	7.2	178	459	0.49	0.88	0.38	0.46	(0.36, 0.48)

[a] Turn on voltage at 1 cd/m^2; [b] The maximum brightness corresponding to the current density; [c] The maximum luminous efficiency corresponding to the current density.

Research Highlights

- Two blue-emitting fluorophore chromophore-functionalized dinuclear platinum (II) complexes were synthesized and characterized.
- The optophysical and electroluminescent properties of the platinum (II) complexes were investigated.
- Near-white emission was observed in its doped single-emissive-layer WPLEDs.
- A maximum brightness of 559 cd/m^2 with a luminance efficiency of 1.12 cd/A was achieved in SEL-PLEDs.